AUTOMATIC CONTROLLED VIBRATORY PILE DRIVING WITH SHOCK-STRESS LIMITATION

D. Reusch

Institute for Construction Management and Machinery
University of Karlsruhe, Germany
email: dirk.reusch@debitel.net

Abstract: For several decades vibratory pile driving has been extensively applied in civil engineering, e.g. in the construction of bulkheads. On urban construction sites shock waves occur which could damage nearby building structures and annoy humans. State-of-the-art machinery provides three control inputs (frequency, excitation force and surcharge force) to achieve two almost contradictory goals: fast pile penetration and shock stress below given limits (e.g. by DIN 4150). A nonlinear model explains the impact of all three control inputs on the quasi-stationary pile movement, such as penetration rate and oscillation amplitude. A fuzzy conntroller based on quantitative model-derived relations between control inputs and penetration rate is designed and implemented. In a second step the fuzzy controller is extended by an shock-stress limiting component

Keywords: vibratory pile driving; shock-stress limitation; nonlinear oscillation; fuzzy control

1 INTRODUCTION

In the following we refer to the pile driving system as shown in Fig. 1. Pile head and vibrator are rigidly connected. They resemble a rigid body with mass

$$m_d = m_e + m_p. \tag{1}$$

A vibration isolated guide block allows the application of an additional surcharge load. Altogether we have the surcharge load

$$F_{a,g} = F_a + m_d g. \tag{2}$$

Inside the vibrator unbalanced rotating masses generate a harmonic oscillating, vertical excitation force

$$F_e(t) = \hat{F}_e \sin(\Omega t + \psi). \tag{3}$$

Pile oscillation often decreases shaft friction and thus eases penetration. An irreversible motion downwards is induced by the surcharge load depending on the sum of all soil reaction forces F_b.

Increasing penetration depth and different soil layers are constantly changing the system behaviour. These changes could be tracked by varying the control inputs (Ω, F_a, and $\hat{F}_e$) to maximize penetration rate and limit shock-stress in the environment.

2 PILE DRIVING PROCESS

2.1 *Dynamic of Rigid Bodies*

The system of Fig. 1 has two degrees of freedom. For a sufficient small observation period and steady state oscillation the position of the guide block can described as

$$y(t) \approx vt, \tag{4}$$

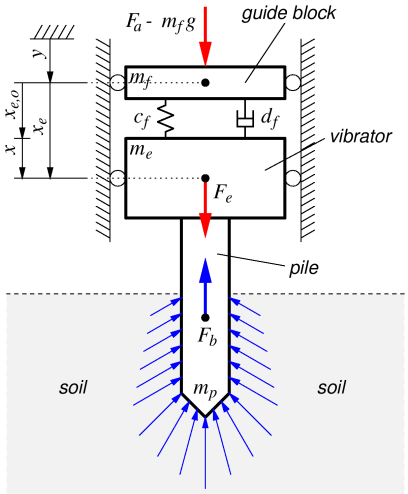

Figure 1: Pile Driving System.

where v is the penetration rate. For the elongation x from the position of equilibrium $x_{e,0}$ the principle of D'ALEMBERT yields

$$m_d \Omega^2 x'' + d_f \Omega x' + c_f x + F_b(z, z') = F_{a,g} + F_e(\tau). \tag{5}$$

F_b shall depend on the absolute position and velocity

$$z = x + y,\ z' = x' + y'. \tag{6}$$

$\tau = \Omega t$ is a dimensionless time and "'" denotes "$\frac{d}{d\tau}$". Solutions of eq. (5) can be subharmonic or even chaotic [1][2]. In this paper we are only interested in 2π-periodic solutions $x(\tau)$ and therefore consider F_b also to be 2π-periodic. Averaging both sides of eq. (5), we get

$$F_{a,g} = \frac{1}{2\pi} \int_0^{2\pi} F_b d\tau. \tag{7}$$

This equation describes implicitly the influence of the surcharge load on steady-state oscillations governed by eq. (5).

2.2 Pile Motion & Interaction with Soil

A typical pile motion cycle is shown in Fig. 2. A motion downwards is followed by a motion upwards. Reversal of motion occurs at positions z_i, $i = 1, \ldots, 3$. At z_1 the pile tip shall have no soil contact. It hits the soil at z_+ and until z_2 soil deformation and displacement takes place. Between z_2 and z_- the soil is relaxed and the tip looses contact. Certainly tip/soil-

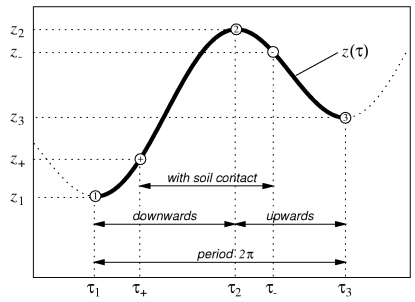

Figure 2: Pile motion cycle.

interaction can also take place without soil contact loss. Different motion types with respect to the soil resistance have been identified [3][1][4]. According to [4] we distinguish:

- *slow vibratory pile driving:* reversal of motion occurs, the soil is relaxed completely, resistance at tip is small compared to penetration by pressing.
- *fast vibratory pile driving:* reversal of motion occurs; soil is not completely relaxed; resistance at tip is larger compared to slow vibratory pile driving.
- *pulsating vibratory pile driving:* no reversal of motion; resistance at tip is larger compared to fast vibratory pile driving.

It is justified to assume periodic solutions of eq. (5) to be approximately harmonic [5], i.e.

$$x(\tau) \approx \hat{x} \sin(\tau). \tag{8}$$

With the definition of a *normalized penetration rate*

$$\nu = \frac{v}{\Omega \hat{x}}, v \geq 0 \tag{9}$$

we can write

$$z(\tau) \approx \hat{x}(\sin \tau + \nu\tau). \tag{10}$$

For $0 \leq \nu < 1$ we have slow or fast pile driving, and $\nu \geq 1$ indicates pulsating vibratory pile driving. Furthermore we define a *soil contact index*

$$\kappa = \frac{z_2 - z_+}{z_2 - z_1}, \text{ for } z_+ \geq z_1, \tag{11}$$

to detect slow ($\kappa < 1$) and fast ($\kappa = 1$) pile driving.

3 SOIL MODEL

Modeling the soil reactions, we use the formulation

$$F_b(z, z') = M(z) + S(z) + d\Omega z'. \tag{12}$$

M corresponds to shearing stress at the shaft. S describes the stress behaviour of the soil under the tip. Wave radiation at shaft and tip is taken into account by a linear viscous damping term $d\Omega z'$.

3.1 Shaft Friction

The shaft friction force can be modeled with

$$M' = \alpha z' \left(1 - \frac{M}{M_{max}} \operatorname{sign}(z')\right). \tag{13}$$

This is a simplification of a model proposed in [4]. M_{max} and α are model parameters. M_{max} is the absolute value of the totally mobilised friction force. The ratio $\frac{\alpha}{M_{max}}$ determines the slope of $M(z)$ with respect to z. In the limit $\frac{\alpha}{M_{max}} \to \infty$ eq. (13) represents COULOMB-friction.

3.2 Tip Force

We assume, that the soil under the tip has ideal elastic and plastic properties. This leads to

$$S(z) = S_{max} \begin{cases} \frac{z - z_+}{\Delta z} & ; \quad z_+ \leq z < z_+ + \Delta z \\ 1 & ; \quad z_+ + \Delta z \leq z < z_2 \\ \frac{z - z_-}{\Delta z} & ; \quad z_- = z_2 - \Delta z \leq z \leq z_2 \\ 0 & ; \quad \text{else} \end{cases}. \tag{14}$$

S_{max} and Δz are model parameters. When the tip force reaches S_{max} plastic deformation starts. The elastic stiffness is given by $\frac{S_{max}}{\Delta z}$.

4 PENETRATION RATE

From eq. (9) we get the penetration rate as

$$v = \nu \Omega \hat{x}. \tag{15}$$

Solving eq. (5) with the method of harmonic balance [6][7] gives $\Omega(\hat{x}, \nu)$. In general, a multi-valued function. For constant $(\hat{x}, \nu)$ always the largest frequency Ω yields a maximal penetration rate v.

In the following sections we discuss the impact of phase shift ψ and soil contact index κ on the penetration rate using model parameters of tab. 1. They depend both on f and $F_{a,g}$, which will be shown in sec. 4.3. The role of the excitation force $\hat{F}_e$ will not be discussed, because it is pretty obvious to use the maximum available for optimal penetration[1].

[1] Under the premise that the system response is not subharmonic or chaotic.

$S_{max} = 80\,\text{kN}$	$c_f = 2\,\text{kN/mm}$
$M_{max} = 20\,\text{kN}$	$d_f = 10\,\text{kNs/m}$
$d = 20\,\text{kNs/m}$	$\hat{F}_e = 45\,\text{kN}$
$\frac{\alpha}{M_{max}} = 500/\text{m}$	$m_d = 1200\,\text{kg}$
$\Delta z = 1\,\text{mm}$	

Table 1: Parameter set used for fig. 3–5.

4.1 Impact of Phase shift

As shown in fig. 3, the maxima of v with respect to ψ are near the backbone curve ($\psi = 90°$). For larger soil contacts the maxima are connected with phase shifts slightly larger than $90°$. Phase shifts $\psi < 90°$ should be avoided, because nonlinear jump phenomena can occur in these region [8].

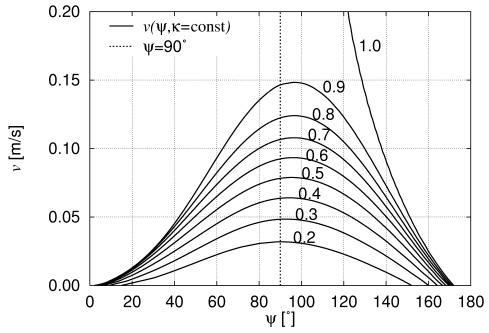

Figure 3: Penetration rate v vs. phase shift ψ.

4.2 Impact of Soil Contact

Fig. 4 illustrates the situation for ψ =const, $\psi \geq 90°$. The larger the soil contact κ the larger is the penetration rate v.

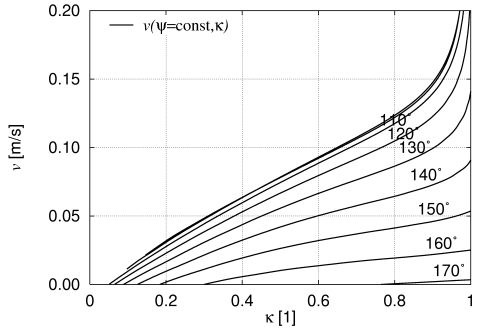

Figure 4: Penetration rate v vs. soil contact index κ.

4.3 Maximisation Strategy

Now we try maximize the penetration rate with respect to the actual control inputs. Fig. 5 shows $F_{a,g}$ as function of f with v, ψ, or κ as parameter. We already know, that we have to choose f and $F_{a,g}$ such that:

1. $\psi \approx 90°$, $\psi \geq 90°$ (e.g. $90° \leq \psi \leq 110°$),
2. $\kappa \approx 1$, $\kappa < 1$ (e.g. $0.85 \leq \kappa \leq 0.95$).

With $f \approx 25$Hz and $F_{a,g} \approx 60$kN a penetration rate $v \approx 0.16 \frac{\text{m}}{\text{s}}$ could be achieved.

Fig. 5 is only valid for a short period of time. Due to increasing friction and damping, we have to expect, that the backbone curve ($\psi = 90°$ is moving towards higher frequencies. Therefore it seems reasonable to give the control of ψ a higher priority than that of κ.

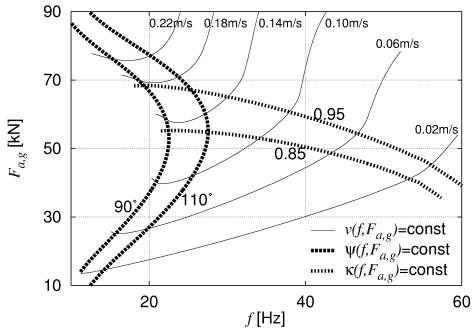

Figure 5: Maximisation of penetration rate v.

5 Shock Stress

Shock waves caused by vibratory pile driving, especially on urban construction sites, are problematic. They can damage nearby building structures and annoy humans. Sensitive technical equipment is destroyed or works faulty. This is the motivation for an automatic shock-stress limitation, which allows maximisation of the penetration rate at the same time.

The prediction of transmission and propagation of shock waves is a quite complex subject. Complete modeling of transmission paths (vibrator/pile/soil/building/shock sensor) requires the estimation or knowledge of a huge amount of parameters. Experience [9][10] shows, that prediction of shock stress, in general, is tainted with large uncertainties [11]. Furthermore the eigen frequencies of many building elements can be found between 10 and 50Hz [12]. A typical frequency range of vibratory pile driving machinery.

5.1 Appropriate Control Quantity

Criteria for shock stress are usually given by national standards (e.g. DIN 4150 Part3, BS 7385 Part 3, SN 640 312a, ...). They impose frequency-dependent or constant limits on the vibration velocities at prescribed measuring points.

In many cases, multiple shock stress signals $e_1, \ldots, e_n$ have to be monitored for a frequency range $[\omega_a, \omega_b]$. With the corresponding limits $E_{i,max}(\omega)$, we define the *maximal shock stress*

$$\varepsilon = \max_{i \in \{1,\ldots,n\}} \left\{ \max_{\omega \in [\omega_a, \omega_b]} \left(\frac{|E_i(j\omega)|}{E_{i,max}(\omega)} \right) \right\}. \quad (16)$$

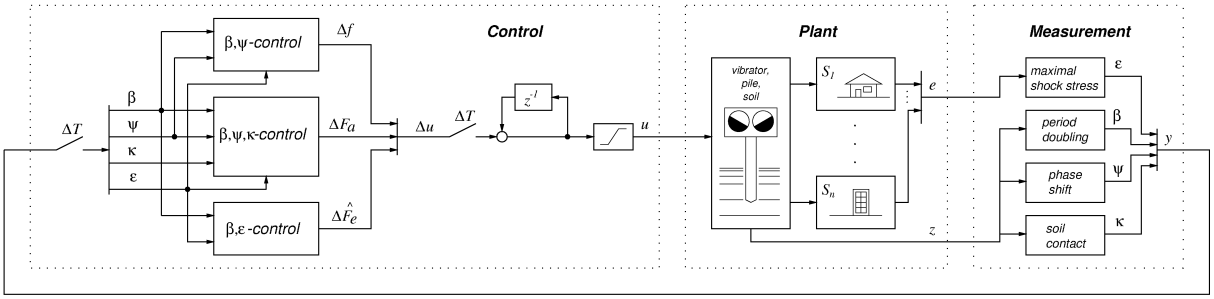

Figure 6: Closed control loop with fuzzy controller.

$E_i(j\omega)$ is the FOURIER-transformed of e_i. For $\varepsilon \leq 1$ no limit is exceeded. $\varepsilon > 1$ indicates, that at least one limit is exceeded. E.g. $\varepsilon = 1.2$ means, that at least one signal is 20% larger than allowed.

5.2 Limitation Strategy

If we are near the limits or, even worse, already beyond the permissible, then control input changes must not increase shock stress. Modeling of multiple transmission path seems in general to be not viable. We make only one, quite general, assumption: on every transmission path there is, to some degree, dissipation of energy. The energy put into the whole is bound by the excitation force $\hat{F}_e$. That leads to rather simple strategy: to decrease shock stress we decrease $\hat{F}_e$ and vice versa. This approach seems to be trivial, and we have to expect $\hat{F}_e = 0$, i.e. the vibrator will be switched off. But in conjunction with the strategy of sec. 4.3 it will prove its power.

6 FUZZY CONTROLLER

Fig. 6 shows the fuzzy controller [13][14] in the closed control loop. It works time discrete with $\Delta T \approx$ 1s.

6.1 Inputs/Outputs

From the physical measurements the following controller inputs or control quantities were computed:

- maximal shock stress ε (eq. (16)),
- index to detect period doubling β [5],
- phase shift ψ,
- and soil contact index κ (eq. (11)).

The outputs of the controller are changes of frequency Δf, static load ΔF_a and excitation force $\Delta \hat{F}_e$.

6.2 Knowledge Base

Maximum penetration rate and limited shock stress are in general contradictory goals. Shock-stress limitation must have precedence over all other control goals. Resolution of this conflict is done by a priority list:

1. shock-stress limitation ($\varepsilon \leq 1$).
2. avoidance of damages to machinery ($\beta \approx 0$).
3. large oscillation amplitude $\hat{x}$ ($\psi \approx 90°$).
4. slow vibratory pile driving with maximal penetration rate v ($\kappa \approx 1$, $\kappa < 1$).

control input	control quantity			
f, F_a, $\hat{F}_e$	ε	β^2	ψ	κ
$f \uparrow$	–	↘	↗	–
$f \downarrow$	–	↗	↘	–
$F_a \uparrow$	–	↘	↘	↗
$F_a \downarrow$	–	↗	↗	↘
$\hat{F}_e \uparrow$	↗	↗	–	–
$\hat{F}_e \downarrow$	↘	↘	–	–

Table 2: Relations between control inputs and quantities ("–" not used).

The quantities ε, β, ψ and κ are controlled by f, F_a and $\hat{F}_e$ using the relations listed in tab. 2.

6.3 Design and Tuning

We formulated rule bases consisting of "IF ... THEN ..."-rules for each controller output. Not shown in fig. 6, we use additional inputs: $\Delta\varepsilon(t) = \varepsilon(t) - \varepsilon(t - \Delta T)$ and $\Delta\psi(t) = \psi(t) - \psi(t - \Delta T)$ [15]. The fuzzy partitions consist of 5 (ε), 4 ($\Delta\varepsilon$), 2 (β), 3 (ψ),3 ($\Delta\psi$), and 3 (κ) primary fuzzy sets. For the output ranges of Δf, ΔF_a, and $\hat{F}_e$ fuzzy-singletons are used. The rule bases contain 28 ($\beta\,\psi$-control), 20 (β, ψ, κ-control), and 39 (β, ε-control) rules.

Fuzzy inference is performed with the algebraic product as conjunction and implication operator. Rule accumulation is done with the algebraic sum and defuzzification with the COS method [14]. For tuning purposes each controller output can be scaled by a factor.

7 RESULTS

Three different piles and two shock sensors (measuring in $x-$, $y-$ and $z-$direction) were used in large-

[2] Relations concerning β are taken from [2] and [5].

scale experiments at our test site near Karlsruhe [16]. Parameters for the results presented below are listed in tab. 3.

m_e	$= 1200\,\text{kg}$	pile: tubular steel (diam. 10/12cm)
f	$= 20 \ldots 40\,\text{Hz}$	with solid cone tip; m_p=195kg
F_a	$= 0 \ldots 25\,\text{kN}$	soil[3]:sand (depth <3–4m),
$\hat{F}_e$	$= 0 \ldots 47\,\text{kN}$	pebbles (depth >3–4m)

Table 3: Large-scale experiment parameters.

7.1 Maximisation of Penetration Rate

Fig. 7a shows penetration depth vs. time of several experiments with constant control inputs. Only with 30Hz a depth of 5m was reached after ≈ 150s. Using 20Hz, the process got stuck ≈ 4m, and with 40Hz not even 2m were achieved.

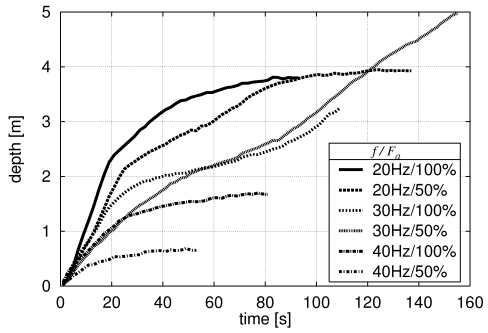

(a) without automatic control

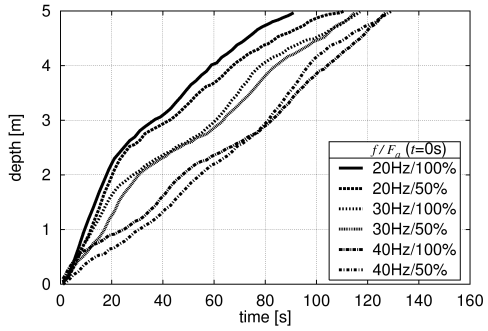

(b) with automatic control

Figure 7: Depth vs. time in experiments without (a) and with (b) automatic control.

Fig. 7b shows the corresponding results using automatic control. The initial values of the control inputs were the same as in fig. 7a. In each case a depth of 5m was reached faster.

[3]Details about soil are given in [4] and [5].

7.2 Shock-Stress Limitation

Shock stress on the ground was measured 6m (sensor I) and 12m (sensor II) apart from the pile. Fig. 8 shows the results of an experiment with in comparison to a corresponding experiment without shock-stress limitation. Without limitation, a depth of 5m was reached after $\approx 80s$. At a depth of ≈ 2.5m at least one limit was exceeded by 40%. With limitation, only minor excesses $\approx 5\%$ were detected and it took ≈ 260s to reach the final depth.

To prove the robustness of the controller one shock sensor was mounted on a pedestal, which had very low damped resonance frequencies at 19, 16, and 25Hz in x-, y-, and z-direction [16]. As a "worst case" we chose an initial frequency of 20Hz and maximal excitation force. Thus the controller had to start near one resonance frequency (19Hz) and to drive through another (25Hz) in order to reach a depth of 5m.

In Fig. 9 the results are shown. Without limitation, a depth of 5m was reached after ≈ 80s. At least one limit was exceeded by up to 700%.

With shock-stress limitation, the controller initially had to decrease the excitation force to zero. That stopped the driving process. Then the gradually increasing excitation frequency came near the next resonance frequency (25Hz). Again, the excitation force was decreased to zero (between 60s and 80s). However, at least one limit was exceeded by $\approx 500\%$. After 150s the resonance frequency (25Hz) was finally left behind and the pile was driven ≈ 3.5m in ≈ 80s

In this worst case, the controller could not prevent significant limit excesses. The first excess at the beginning was inevitable. Because the initial frequency and excitation force were chosen inappropriate. During the second, the controller drove through an unknown resonance frequency (25Hz) with an excitation force of zero, i.e. the vibrator was practically switched off. But in reality, due to manufacturing tolerance of the vibrator, there was still a small excitation force ($\approx$ 2kN) active. Which was enough to excite the very low damped pedestal carrying one shock sensor.

8 CONCLUSIONS

It has been shown that the vibratory pile driving process can be optimized using an automatic controller with respect to the penetration rate and environmental shock stress. A very simple shock stress limitation strategy performed reasonably well, even in worst cases. For further developments, it will be necessary to have a more powerful prototype, which could be used on real construction sites.

ACKNOWLEDGEMENTS

The author wishes to acknowledge the financial support by the Deutsche Forschungsgemeinschaft, Bonn, Germany.

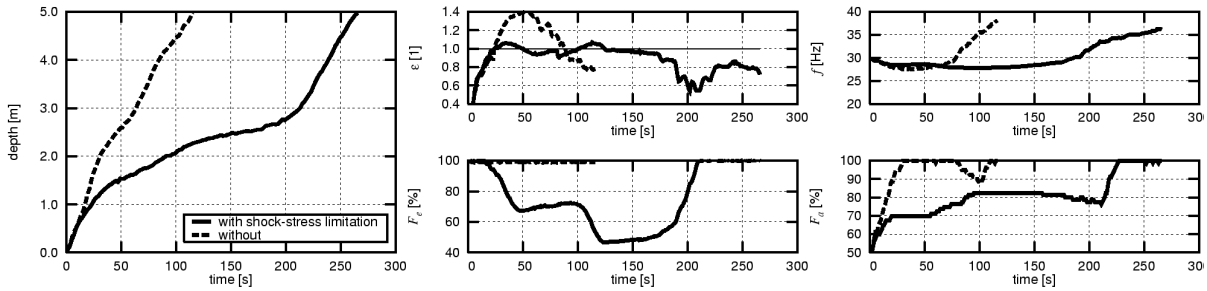

Figure 8: Depth, maximal shock stress and control inputs ($E_{\mathrm{I},max} = 8\frac{\mathrm{mm}}{\mathrm{s}}$, $E_{\mathrm{II},max} = 6\frac{\mathrm{mm}}{\mathrm{s}}$).

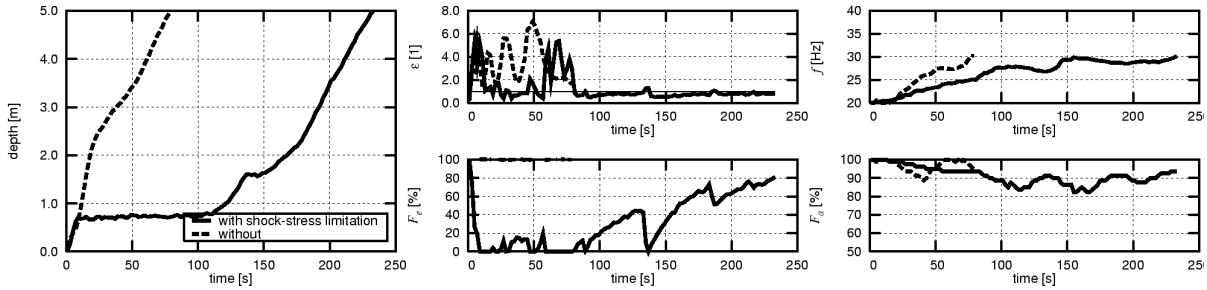

Figure 9: Depth, maximal shock stress and control inputs in a "worst case" ($E_{\mathrm{I},max} = 12\frac{\mathrm{mm}}{\mathrm{s}}$, $E_{\mathrm{II},max} = 12\frac{\mathrm{mm}}{\mathrm{s}}$).

REFERENCES

[1] Verspohl, J., *Ungefesselte hysteretische Systeme unter besonderer Berücksichtigung der Vibrationsrammung*, Ph.D. thesis, Universität Karlsruhe, 1990.

[2] Storz, M., *Stabilität der Bewegungen eines Reibschwingers mit Stoß am Beispiel des Vibrationsrammens*, Ph.D. thesis, Universität Karlsruhe, 1994.

[3] Rogder, A. A.; Littlejohn, G. S., "A study of vibratory driving in granular soil", *Geotechnique*, vol. 30, no. 3, pp. 269–293, 1980.

[4] Dierssen, G., *Ein bodenmechanisches Modell zur Beschreibung der Vibrationsrammung in körnigen Böden*, Ph.D. thesis, Universität Karlsruhe, 1994.

[5] Oleff, A., *Auslegung von Stellelementen für Schwingungserregerzellen mit geregelter Parameterverstellung und adaptive Regelungskonzepte für den Vibrationsrammprzeß*, Ph.D. thesis, Universität Karlsruhe, 1996.

[6] Gelb, A.; Vander Velde, W. E., *Multiple-Input Describing Functions and Nonlinear System Design*, McGraw-Hill, New York, San Francisco, London, 1968.

[7] Föllinger, O., *Nichtlineare Regelungen I*, R. Oldenbourg, München, Wien, 6th ed., 1991.

[8] Ehrich, F.; Abramson, H. N., "Nonlinear Vibrations", in "Shock and Vibration Handbook", (edited by C. M. Harris), McGraw-Hill, 1996.

[9] Niederwanger, G.; Majer, J., "Measurement and Estimation of Vibrations of Constructions Caused by Vibrators", *Österreichische Ingenieur- und Architekten-Zeitschrift*, vol. 134, no. 7/8, pp. 410–414, 1989.

[10] Schuppener, B., "Eine Proberammung vor einer Stützwand mit unzureichender Standsicherheit", *Mitteilungsblatt der Bundesanstalt für Wasserbau*, , no. 72, pp. 38–47, 1995.

[11] Pallocks, W.; Zierach, R., "Zum Problem der Prognose von Schwingungen und Setzungen durch Pfahlrammungen mit Vibrationsbären", *Mitteilungsblatt der Bundesanstalt für Wasserbau*, , no. 72, pp. 48–55, 1995.

[12] Müller-Boruttau, F. H., "Erschütterungen beim Spundwandbau: Einwirkung auf Menschen, Bauwerke und technische Einrichtungen", *Bauingenieur*, vol. 71, pp. 33–39, 1996.

[13] Lee, C. C., "Fuzzy Logic in Control Systems: Fuzzy Logic Controller", *IEEE Transactions on Systems, Man, and Cybernetics*, vol. 20, no. 2, pp. 404–435, 1990.

[14] Kiendl, H., *Fuzzy Control methodenorientiert*, R. Oldenbourg Verlag, München, 1997.

[15] Tang, K. L.; Mulholland, R. J., "Comparing Fuzzy Logic with Classical Controller Designs", *IEEE Transactions on Systems, Man, and Cybernetics*, vol. SMC-17, no. 6, pp. 1085–1087, 1987.

[16] Gehbauer, F.; Reusch, D., "Abschlußbericht zum DFG-Projekt Ge 577/9-1", Tech. rep., Institut für Maschinenwesen im Baubetrieb, Universität Karlsruhe, 2000.